JOURNAL OF MATERIALS SCIENCE 9 (1974) 725–736

Development of a general surface contour by ion erosion. Theory and computer simulation

J. P. DUCOMMUN, M. CANTAGREL, M. MARCHAL*
Thomson-CSF, Laboratoire Central de Recherches, 91401 Orsay, France

An analytical treatment of the development of a general contour under ion bombardment is proposed. The derived equations relate the properties of the eroded material through its yield variation upon the angle of incidence, $S(\theta)$. New specific angles (θs_1 and θs_2) are introduced which limit regions where the evolution process of the surface may be different. The theory allows prediction of the number of angular points which will appear in each region.

A computer simulation program is used to describe the evolution of sine-type surfaces. With infinite time, such profiles in relief above a horizontal plane, tend towards the steady state which exists in a horizontal plane. The model is compared to one previously described.

1. Introduction

Changes in surface topography of solid surfaces eroded by a low energy ion beam have often been reported. Stewart and Thompson [1], assuming that the dependence of the sputtering yield S on the angle of incidence θ could possibly be responsible for the observed microscopic surface features, were the first to give the equations of motion of the intersection of two planes during erosion. These results, applied to the erosion of a step, show the dominant role played by the planes inclined at an angle θ_p corresponding to the angle where the sputtering yield is maximum.

Using the same basic assumptions, Nobes *et al* [2, 3] developed a theory for the sputtering of amorphous solids by an ion beam and the changes in surface topography to which this sputtering leads. This model shows that a steady state is reached when the surface topography consists of planes aligned either parallel or perpendicular to the direction of the ion beam and inclined at $\pm\ \theta_p$ to the horizontal. Using the small displacements method, the same authors [4] have given an analytical treatment of surface profile, then a computer simulation was devised to model the development of a sinusoidal surface by iterations.

It was then of prime interest to find some non-iterative method of following the development of a general surface contour. Thus, using the same form of $S(\theta)$, we have developed a new model to predict the surface evolution with time. A computer simulation program was established by which means the evolution of a general surface contour subjected to ion bombardment can be drawn at any time using the non-iterative method.

This computer simulation was applied to several different suface contours and the results are discussed.

2. Analytical treatment of the development of a surface contour

2.1. Theory

The fundamental hypotheses are the following.

1. For simplicity we consider the erosion of a surface contour (C) lying in the (xoy) plane and represented by the equation $y = f(x, o)$.

2. The bombarded material is homogeneous and isotropic.

3. Planes (assumed as straight lines in the model) move parallel to themselves by erosion.

4. Secondary effects, such as defects introduced by ion bombardment, redeposition of

Present address: LCC-CICE, 21000 Dijon, France.

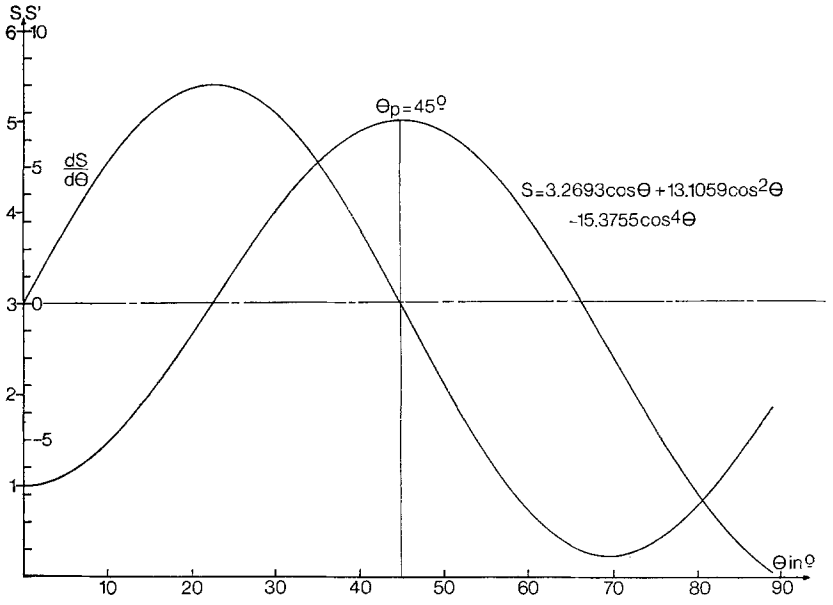

Figure 1 Variation of sputtering with angle of incidence.

sputtered materials, diffusion, etc, will not be considered.

5. The variation of S with θ is a function which has the form shown by Fig. 1. S is S_0 for normal incidence, ($\theta = 0$), increases up to a maximum at $\theta = \theta_p$ and decreases to $S = 0$ at $\theta = 90°$.

Let us consider that (C), $y = f(x, o)$ is the envelope of a family of straight lines (D) described by:

$$y - xf'(x_i) + x_i f'(x_i) - f(x_i) = 0 \qquad (1)$$

where x_i, $y_i = f(x_i)$ is an arbitrary point of C.

The family of straight lines (D') transformed from the family (D) by the ion beam erosion is:

$$y - xf'(x_i) + x_i f'(x_i) - f(x_i) + A(x_i) = 0 \quad (2)$$

where $A(x_i)$ is the displacement of a straight line (D) parallel to itself.

Introducing the parameters that govern the ion-beam erosion, $A(x_i)$ can be expressed as:

$$A(x_i) = A[\theta(x_i)] = \frac{\phi}{n} tS(\theta) \qquad (3a)$$

with $\tan\theta = f'(x_i)$ and $-\pi/2 < \theta < \pm\pi/2$, (3b)

where ϕ = ion flux ($cm^{-2}\ sec^{-1}$) in the negative oy direction, n = atomic density of the target in atoms cm^{-3}, t = time in sec, S = sputtering yield in atoms per incident ion.

The new surface contour (C') is the envelope of (D') and is given by solution of the system of equations:

$$\begin{cases} y - xf'(x_i) + x_i f'(x_i) - f(x_i) + A(x_i) = 0 & (4) \\ -xf''(x_i) + x_i f''(x_i) + \dfrac{\delta A(x_i)}{\delta x_i} = 0 & (5) \end{cases}$$

Equation 5 is equivalent to:

$$x = x_i + \frac{1}{f''(x_i)} \frac{\delta A(x_i)}{\delta x_i} \qquad (6)$$

Substituting Equations 3a and b into Equations 6 and 4 leads to:

$$x = x_i + \frac{\phi}{n} t \cos^2\theta \frac{dS(\theta)}{d\theta} \qquad (7)$$

$$y = f(x_i) + \frac{\phi}{n} t \left[\sin\theta \cos\theta \frac{dS(\theta)}{d\theta} - S(\theta) \right]. \qquad (8)$$

Equations 7 and 8 are parametric equations of (C').

2.2. Discussion

This model and the proposed analytical treatment avoid iterative calculus to obtain the curve (C') at any time t.

According to Equations 7 and 8, at any (x_i, y_i) point of (C) there corresponds a point on (C'). In such a mathematical treatment, the angles θ measured on (C) are preserved on (C'). Later, we will see that, physically speaking, some points

(x,y) of the transformed curve disappear. x and y are linearly dependent on t and ϕ/n, and also depend on the angle of incidence θ, explicitly through the trigonometric functions of θ ($\cos^2\theta$ or $\sin\theta\cos\theta$) and implicitly through the variation of S' and S with θ. Several particular cases may be observed.

(a) A translation in direction y only is obtained if:

$$\phi/n\, t \cos^2\theta \frac{dS(\theta)}{d\theta} = 0 \qquad (9)$$

that is:

$$\text{either } \cos\theta = 0 \quad \theta = \pi/2$$

$$\text{or } \frac{dS(\theta)}{d\theta} = 0 \quad \begin{cases} \theta = 0 \\ \theta = \theta_p \\ S(\theta) = \text{constant} \quad \forall\theta \end{cases}$$

Those conditions are equivalent to the conditions found by Nobes *et al* [2, 3] using a different analytical approach.

(b) The contour will remain unchanged if

$$\frac{\Delta y}{\Delta x} = b \quad \forall\theta$$

$$\frac{\Delta y}{\Delta x} = \tan\theta - \frac{1}{\cos^2\theta}\frac{S(\theta)}{dS(\theta)/d\theta} = b \quad \forall\theta \qquad (10)$$

where b is a constant and $S(\theta)$ should be of the form:

$$S(\theta) = K(\tan\theta - b)\,. \qquad (11)$$

(c) A translation on the x-axis alone will be obtained if:

$$\frac{\phi}{n} t\left[\sin\theta\,\cos\theta\frac{dS(\theta)}{d\theta} - S(\theta)\right] = 0\,. \qquad (12)$$

This is a particular case of (b) where:

$$\frac{\Delta y}{\Delta x} = 0$$

then $b = 0$ and $S(\theta) = K\tan\theta$.

Generally, the translations along x and y occur simultaneously. So it becomes necessary to study (C') as defined by Equations 7 and 8 to follow the development of the surface contour and to predict the existence of cusps and double points.

Cusps, when existing are given by:

$$\frac{dx}{dx_i} = 1 + \frac{d[\Delta x(x_i)]}{dx_i} = 0 \qquad (13)$$

$$\frac{dy}{dx_i} = f'(x_i) + \frac{d[\Delta y(x_i)]}{dx_i} = 0 \qquad (14)$$

Equations 13 and 14 are interdependent and lead to:

$$\frac{\phi}{n} t\left[\cos^2\theta\frac{d^2S(\theta)}{d\theta^2} - 2\sin\theta\cos\theta\frac{dS(\theta)}{d\theta}\right] \qquad (15)$$
$$\cos^2\theta f''(x_i) = -1$$

equivalent to:

$$\frac{\phi}{n} t\left[2\sin\theta\frac{dS(\theta)}{d\theta} - \cos\theta\frac{d^2S(\theta)}{d\theta^2}\right]\frac{f''(x_i)}{|f''(x_i)|} \qquad (16)$$
$$= R(x_i, o)$$

where $R(x_i, o)$ is the radius of curvature of (C).

Equation 16 will be verified if $R(x_i, o)$ and

$$Z(x_i, t) = \frac{\phi}{n} t\left[S\sin\theta\frac{dS(\theta)}{d\theta} - \cos\theta\frac{d^2S(\theta)}{d\theta^2}\right]\frac{f''}{|f''|}$$

are secant.

As $R(x_i, o) \geqslant 0$ the intersection between $R(x_i, o)$ and $Z(x_i, t)$ will possibly occur if $Z(x_i, t) > 0$.

Let us designate:

$$Z^*(\theta) = 2\sin\theta\frac{dS(\theta)}{d\theta} - \cos\theta\frac{d^2S(\theta)}{d\theta^2}$$

with $\theta \in [-\pi/2, +\pi/2]$, S being defined in this interval.

Let us analyse the function $Z^*(\theta)$. If $S(\theta)$ is of the general form described by Fig. 1, the function $Z^*(\theta) = 0$ has two roots θs_1 and θs_2 ($\theta s_2 > \theta s_1$), $Z^*(\theta)$ being positive between θs_1 and θs_2 and negative elsewhere. The angle θ_p corresponding to the maximum of $S(\theta)$ is always between the roots θs_1, θs_2 (Fig. 2).

For a given contour (C) described by the Equation $y = f(x, o)$, the slope of the tangents of the curve may vary between two values θ_m and θ_M. Then the function $Z^*(\theta)$ associated with this given curve (C) is to be studied in this interval $[\theta_m, \theta_M]$. The change in the algebraic sign of the function $Z^*(\theta)$ in the interval $[\theta_m, \theta_M]$ depends whether θs_1 and θs_2 are included or not in this interval.

The algebraic sign of $Z(x_i, t)$ is finally dependent on that of $Z^*(\theta)$ and on that of $f''(x_i)$. The following example gives the complete analysis of the different possible intersections between $R(x_i\, o)$ and $Z(x_i\, t)$ in the case of (C) defined by $y = a\sin x$.

The cusps, when they exist, can be associated in pairs. Each pair of cusps gives rise to a double point.

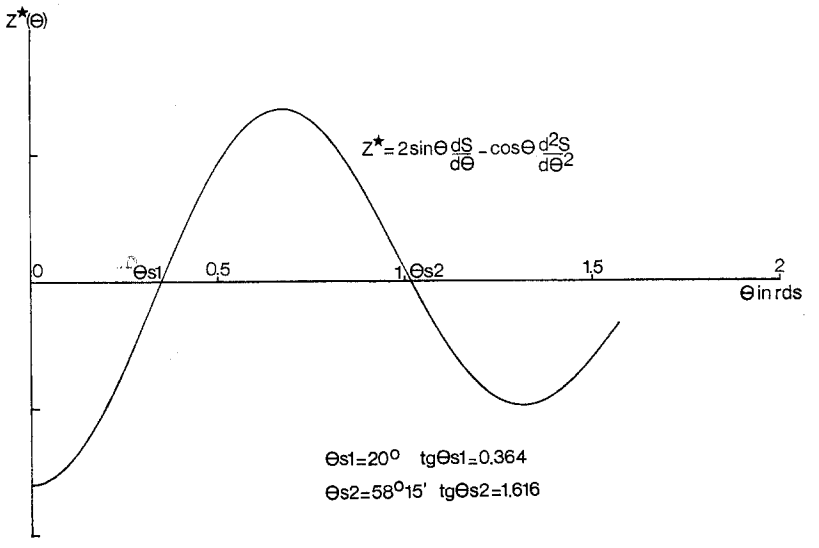

Figure 2 Variation of $Z^*(\theta)$ versus the angle of incidence.

3. Application to a contour represented by $y = a \sin x$

$$x \in [-\pi/2, 3\pi/2]$$

3.1. Starting form of $S(\theta)$

Taking $S(\theta) = 3.2696 \cos\theta + 13.1059 \cos^2\theta - 15.3755 \cos^4\theta$ as already presented by Carter *et al* [4]. $S(\theta)$ is maximum for $\theta_p = 45°$. $Z^*(\theta)$ is represented by Fig. 2. $Z^*(\theta)$ is zero for $\theta s_1 = 20°$ and $\theta s_2 = 58°15$. The maximum inclination θ_M of the function $y = a \sin x$ is given by $\tan\theta_M = a$. For $x = 0$ the algebraic sign of $f''(x)$ changes and $f''(x) < 0$ when $x > 0$.

3.2. Existence of cusps

The intercepts of the function $Z^*(\theta)$ being:

$$\theta s_1 = 20° \qquad \tan\theta s_1 = 0.364$$
$$\theta s_2 = 58°\,15' \qquad \tan\theta s_2 = 1.616$$

Three possibilities occur:

(a) $\theta_M < \theta s_1$
(b) $\theta s_1 < \theta_M < \theta s_2$
(c) $\theta s_2 < \theta_M$.

They can be represented by:

$$y = 0.1 \sin x \quad (\tan\theta_M = 0.1)$$
$$y = \sin x \quad (\tan\theta_M = 1)$$
$$y = 5 \sin x \quad (\tan\theta_M = 5).$$

Table I summarizes the occurrence of the intersections between $R(x_i, o)$ and $Z(x_i, t)$. Figs. 3 to 5 represent the graphical intersections. Thus we find:

$y = 0.1 \sin x$: one possible intersection zone (Table Ia) that is represented in Fig. 3 by two points about the axis $x = \pi/2$. Then (C') will show two cusps in the interval $x \in [-\pi/2, 3\pi/2]$;

$y = \sin x$: three possible intersection zones (Table Ib) Fig. 4 show that there are three pairs of points symmetrical about the axis $x = \pi/2$. Then (C') will show six cusps in the interval $x \in [-\pi/2, 3\pi/2]$;

$y = 5 \sin x$: five possible intersection zones (Table Ic). As shown by Fig. 5, there are, in fact, ten intersections in symmetrical pairs about the axis $x = \pi/2$. (C') will show ten cusps.

3.3. Double points

Following previous results we should have:

– one double point on the y-axis for $y = 0.1 \sin x$;

– three double points, one on the y-axis and two symmetrical points for $y = \sin x$.

– five double points, one on the y-axis, the others in symmetrical pairs for $y = 5 \sin x$.

3.4. Note

The mathematical analysis of double points and cusps predicted more features than we expected. A physical interpretation of these points showed that the extra features disappear when a time parameter is introduced. This will now be discussed.

TABLE I Possibilities of intersections between the curves $R(x_i, o)$ and $Z(x_i, t)$ for $y = a \sin x$ (the zones where intersections can occur are enclosed in a thick line, cross-hatched regions correspond to the zones where the functions $f''(x)$, $Z^*[\theta(x)]$ or $Z(x_i, t)$ are not defined).

(a)

θ	0	θ_M	θ_{s1}	θ_{s2}	$\pi/2$	θ_{s2}	θ_{s1}	θ_M	0	$-\theta_M$	$-\theta_{s1}$	$-\theta_{s2}$	$-\pi/2$	$-\theta_{s2}$	$-\theta_{s1}$	$-\theta_M$	0
f''	+								−	−							+
$Z^*(\theta)$	−	−	+	−	−	+	−	−	−	−	+	−	−	+	−	−	
$Z^*(\theta\|x\|)$	−								−	−							−
$Z(x_i,t)$	−								+	+							−

(b)

θ	0	θ_{s1}	θ_M	θ_{s2}	$\pi/2$	θ_{s2}	θ_M	θ_{s1}	0	$-\theta_{s1}$	$-\theta_M$	$-\theta_{s2}$	$-\pi/2$	$-\theta_{s2}$	$-\theta_M$	$-\theta_{s1}$	0
f''	+	+					−	−	−	−					+	+	
$Z^*(\theta)$	−	+	+	−	−	+	+	−	−	+	+	−	−	+	+	−	
$Z^*(\theta\|x\|)$	−	+					+	−	−	+					+	−	
$Z(x_i,t)$	−	+					−	+	+	−					+	−	

(c)

θ	0	θ_{s1}	θ_{s2}	θ_M	$\pi/2$	θ_M	θ_{s2}	θ_{s1}	0	$-\theta_{s1}$	$-\theta_{s2}$	$-\theta_M$	$-\pi/2$	$-\theta_M$	$-\theta_{s2}$	$-\theta_{s1}$	0
f''	+	+	+			−	−	−	−	−	−			+	+	+	
$Z^*(\theta)$	−	+	−	−	−	−	+	−	−	+	−	−	−	−	+	−	
$Z^*(\theta\|x\|)$	−	+	−			−	+	−	−	+	−			−	+	−	
$Z(x_i,t)$	−	+	−			+	−	+	+	−	+			−	+	−	

4. Contour development

A computer program to solve Equations 7 and 8 was devised allowing one to draw (C′) from (C) using a non-iterative method. Starting from:

$$\frac{\phi}{n} t = \frac{\phi}{n} N t_0 \,, \frac{\phi}{n} t_0 = 5 \times 10^{-2} \text{ cm} \,.$$

N is an integer in the program.

The initial contour is defined by 101 points equally spaced along the x-axis. Fig. 6 shows the results of the application of this program to the curve (C) represented by $y = 0.1 \sin x$. A double point, and two cusps appear for $N \geqslant 7$.

The part of the curve (C′) which contains the cusps over the double point has no physical significance, so the points (x, y) of this part of (C′) vanish. The same phenomena occur when the double point is not on the symmetry axis. So the physical contour (C′) will exhibit corners instead of double points of the mathematical contour.

Then it becomes necessary to add to the initial computer program:

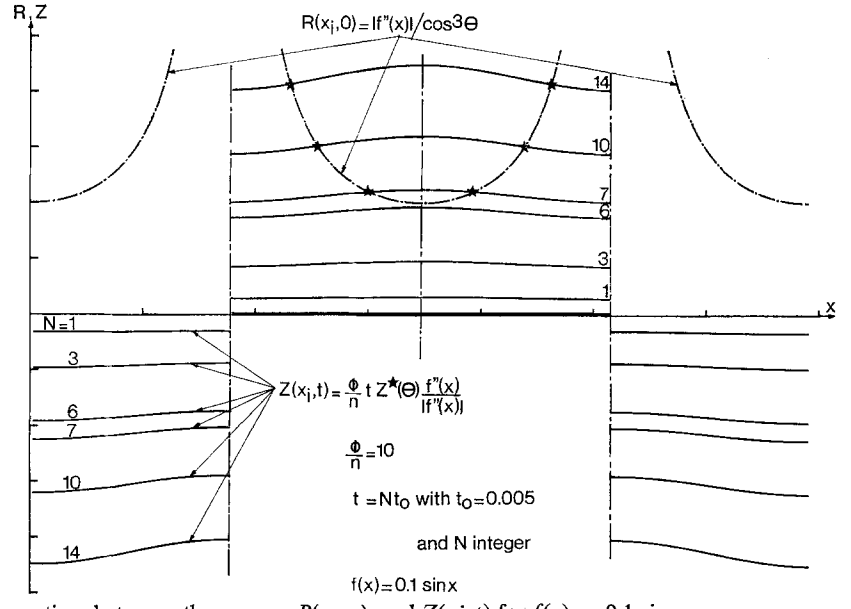

Figure 3 Intersection between the curves $R(x_i, o)$ and $Z(xi, t)$ for $f(x) = 0.1 \sin x$.

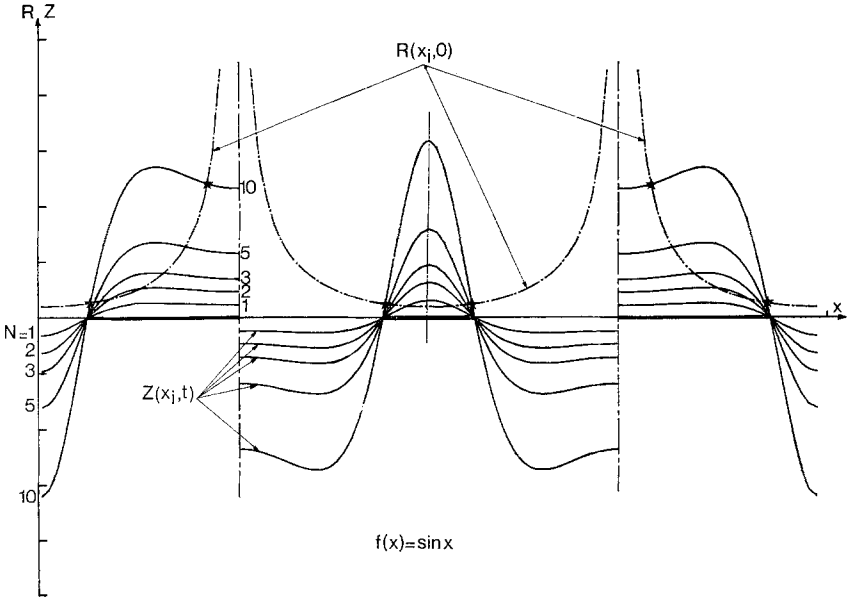

Figure 4 Intersection between the curves $R(x_i, o)$ and $Z(x_i, t)$ for $f(x) = \sin x$.

a program to search for cusps;

a program of calculation of the double points;

a program to strike out the points that have no physical significance.

Using this completed computer program, the results obtained for $y = 0.1 \sin x$ and $y = 5 \sin x$ are shown in Fig. 7.

The general tendency of a sinusoidal contour is to progressively transform into a horizontal straight line, the stages of this evolution being different depending upon the maximum slope θ_M of the original profile.

(1) $\theta_M < \theta s_1$. The evolution toward a horizontal plane occurs in only one step. A corner is created and at this point symmetrical planes vanish.

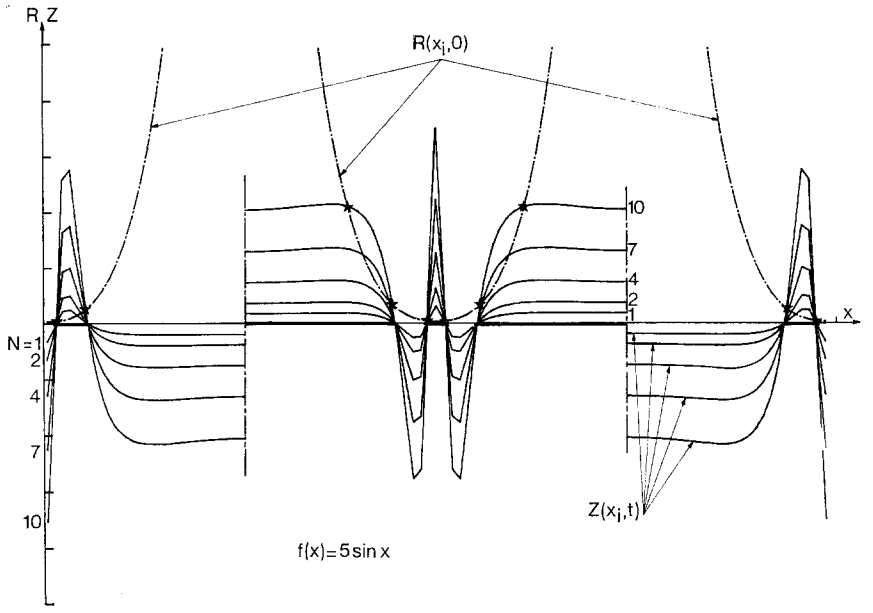

Figure 5 Intersection between the curves $R(x_i, o)$ and $Z(x_i, t)$ for $f(x) = 5 \sin x$.

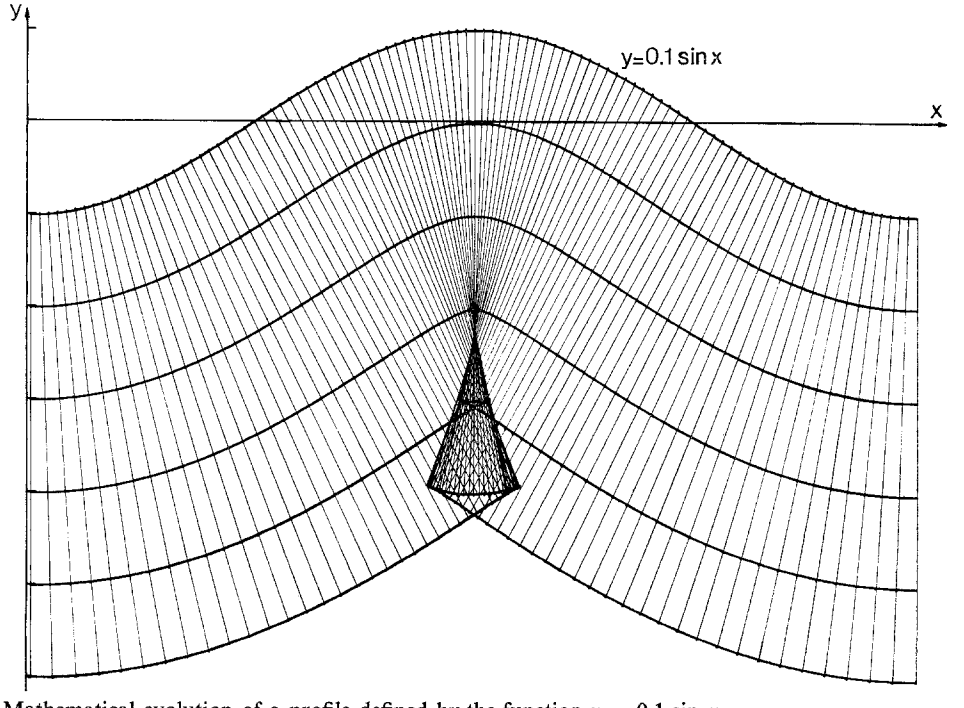

Figure 6 Mathematical evolution of a profile defined by the function $y = 0.1 \sin x$.

(2) $\theta s_1 < \theta_M < \theta s_2$. Two different cases can be expected.

$\theta_M < \theta_p$. The evolution of the profile occurs in two steps: (1) symmetric planes vanish with creation of corner; (2) two other corners appear between the planes with slope θ_M and the planes that have a lower slope. When the planes with slope near θ_M have completely vanished, the behaviour is identical to that of the first case.

$\theta_M > \theta_p$. The same steps occur in the develop-

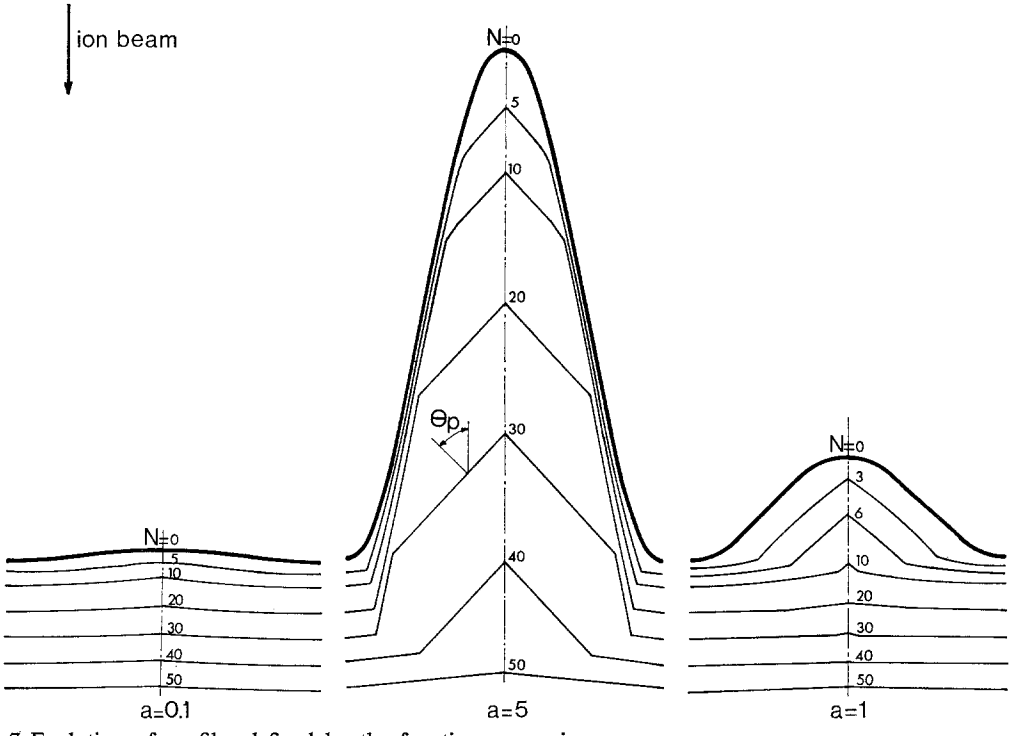

Figure 7 Evolution of profiles defined by the function $y = a \sin x$.

ment of the profile but the role of the planes with slope θ_p is predominant instead of that of planes of θ_M,

(3) $\theta s_1 < \theta s_2 < \theta_M$. Three steps exist: planes with slope θ_p grow at the expense of planes with slope higher than θ_p, two symmetrical corners are created between the planes with slope θ_M and θ_p. When the planes with slope θ_M have vanished the development become identical to (2).

4.1. Time dependence of the existence of angular points

N_c being the lower value of N where all predicted cusps appear on the mathematical transformed contour (C'), Figs. 3 to 5, show that cusps may appear when N_c is high enough. Besides, N_c increases as θ_M approaches through upper values the lower limit of each of the three intervals defined: 0, θs_1, θs_2. N represents the ion beam erosion time, and N_c may be longer than the time of disappearance of the point that generate the corner on the physical contour. Then these points do not appear.

The major consequence of the introduction of time as a physical parameter that governs the appearance of corners is the shift through higher values of the limits between the different expected cases. This shift is a function of the initial contour through its radius of curvature.

5. Discussion

Two new models on the evolution of surface profiles by ion bombardment have been recently published [5, 6]. We make here a comparison between these new approaches and our analytical treatment. In the following sections we compare the theoretical approaches and the results obtained in each of three cases.

5.1. The three models are equivalent

The equivalence between Barber's theory and Carter's theory is demonstrated by Carter *et al* [5]. We can easily show the equivalence between the three models by comparison of Equations 16 and 17 of the study of Carter *et al* [5] and Equations 7 and 8 in our study: these equations are identical.

5.2. Results

While Barber's model is a graphical method, both other studies involve a computer simulation program. Barber's model and our model show that a sinusoidal profile submitted to ion bombardment erodes and leads, with infinite

time, to a horizontal plane. We note that corners appear during erosion.

At this level a difference appears between the results obtained by Catana *et al* [4] and those predicted by both other studies. With the same initial profile, Carter's model leads to a steady state which consists of a triangular pit and a horizontal plateau. The angle of the sides of this triangle is equal to θ^*, where θ^* verifies the relation $S(\theta)^* = S(0)$. These last results are not in agreement with those obtained by others methods. We can show that planes with slope $\pm$ θ^* are not, in fact, a steady state.

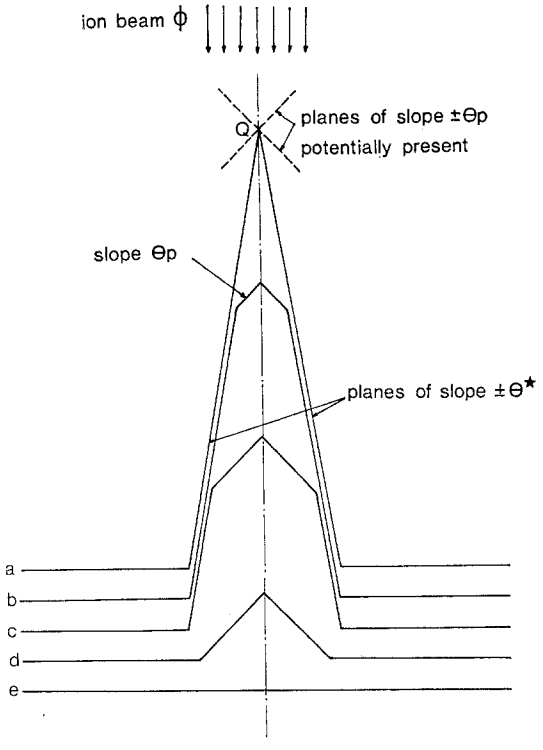

Figure 8 Evolution of a triangular pit by ion erosion.

Let us consider the situation depicted in Fig. 8a. The planes initially present have a slope $\pm$ θ^*. According to Frank's theory [7], planes of intermediate orientations are potentially present at Q. In particular, planes of slope $\pm$ θ_p exist at Q. These planes appear first at the expense of planes of higher slope, as it is shown in our study, and planes of slope $\pm$ θ^* disappear. Then the θ_p planes vanish and the equilibrium topography is also a horizontal plane. The changes in surface topography are depicted in Fig. 8b to e.

5.3. Particular values of θ:θ_p, θs_1, θs_2

Carter *et al* [5] have shown that the angle θ_p, where the sputtering yield is maximum, is corresponding in Barber's model to the point on the erosion slowness curve (other than $\theta = 0$) for which the normal at the polar diagram is parallel to the $1/V$ axis. We show in the Appendix that θs_1 and θs_2 obtained in our study are corresponding to the points of geometrical inflexion on the erosion slowness curve. At these points the angles between the "dissolution trajectories" and the direction of ion beam are extreme. All trajectories are located in the angle formed by these two limiting trajectories, as shown in Fig. 9a, which represents the erosion slowness curve for the empirical form of $S(\theta)$ used by Catana *et al* in their study and in Fig. 9b, which show the erosion of a spherical relief with a maximum slope higher than θs_2.

6. Conclusions

The proposed analytical treatment, the equations and the computer simulation program to which this treatment leads can be applied to any general contour of the form $y = f(x, 0)$; y and its first derivative must be continuous. A general contour, in relief above the horizontal plane, is progressively removed by ion erosion. For infinite values of time, the last stage of the evolution is a horizontal plane normal to the ion beam, this situation being a steady state. The development of such a general contour is strictly dependent of the material subjected to erosion through $S(\theta)$. The position of θ_M regarding the values θs_1 and θs_2, roots of $Z(\theta) = 0$ gives rise, in the example of sinusoidal contour, to three different cases.

(1) $\theta_M < \theta s_1 < \theta_p < \theta s_2$. The steady state is obtained with creation of only one corner.

(2) $\theta s_1 < \theta_M < \theta s_2$ with $\theta s_1 < \theta_p < \theta s_2$. The surface feature is removed with appearance of three corners, one of them on the axis of symmetry, the other two symmetrical about this axis. The maximum slope that can be reached at the corner located on the axis of symmetry is θ_M if $\theta_M < \theta_p$ or θ_p if $\theta_M > \theta_p$.

(3) $\theta s_1 < \theta_p < \theta s_2 < \theta_M$. Five corners, one on the axis of symmetry and the others in symmetrical pairs, appear during evolution towards the horizontal plane. Planes with slope θ_p appear first at the expense of planes of higher slope, then

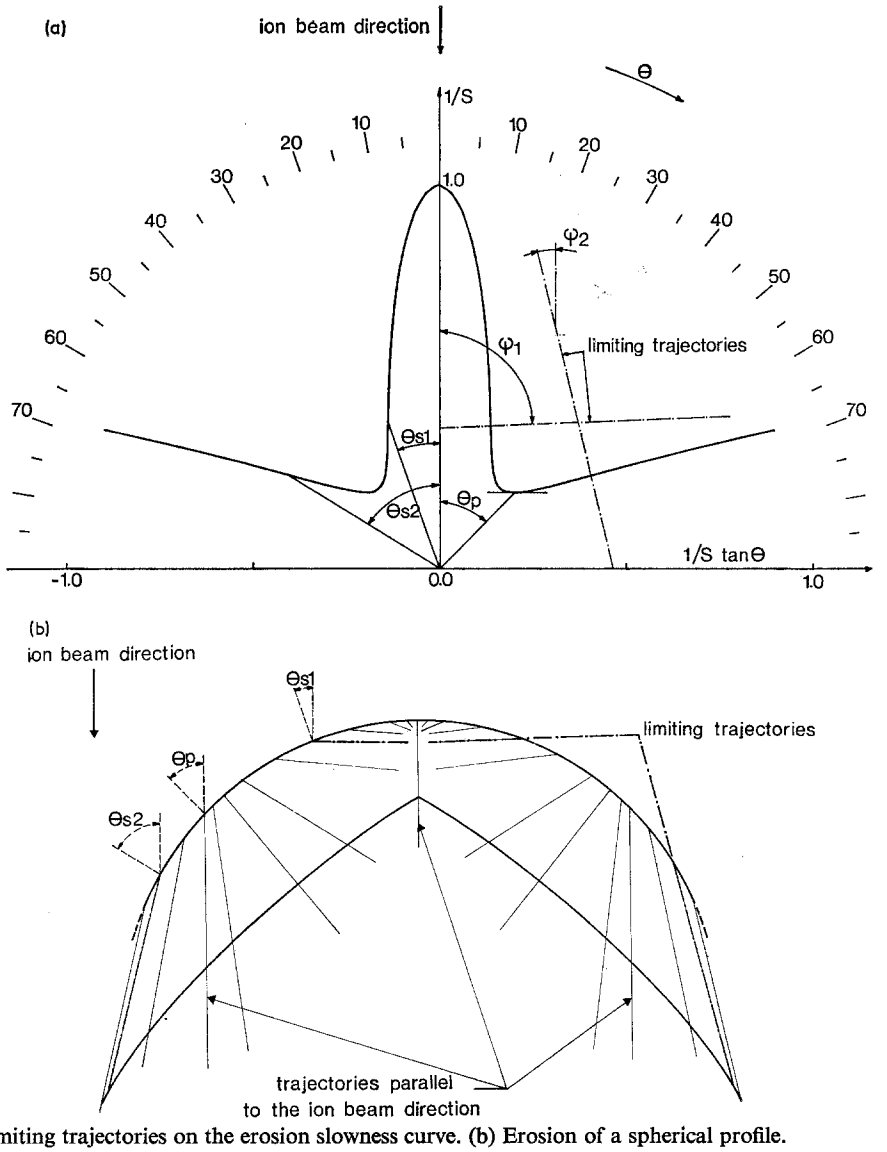

Figure 9 (a) Limiting trajectories on the erosion slowness curve. (b) Erosion of a spherical profile.

these θ_p planes vanish. Planes with slope θ_p are non-stable.

More extensively, a surface contour above a horizontal plane without angular points, subjected to ion erosion transforms into a surface with a predictable number of angular points and tends to a horizontal plane asymptotically with time. The number of angular points depends on the geometry of the contour subjected to erosion (θ_M, R) and on the material through the form of $S(\theta)$.

Three types of planes become predominant in the development of the contour: (1) the horizontal planes that are a steady state position; (2) the vertical planes, remaining unchanged by erosion, and (3) the planes with slope $\pm\ \theta_p$. The three models proposed are shown to be equivalent. The results reported by Catana *et al* are not in agreement with those obtained in both other studies, which lead to identical results. The difference is certainly a consequence of a spurious computational procedure used by Catana *et al*.

Barber *et al*'s model allowed us to propose an additional interpretation of the particular values θs_1 and θs_2 arising in our study.

Appendix

In our study we have found that

$$\Delta x = \frac{\phi}{n} t \frac{dS(\theta)}{d\theta} \cos^2 \theta \qquad (A1)$$

$$\Delta y = \frac{\phi}{n} t \left[\sin \theta \cos \theta \frac{dS(\theta)}{d\theta} - S(\theta) \right] \qquad (A2)$$

$$Z^*(\theta) = 2 \sin \theta \frac{dS(\theta)}{d\theta} - \cos \theta \frac{d^2S(\theta)}{d\theta^2} \cdot \qquad (A3)$$

The sputtering yield, $S(\theta)$, and the sputtering rate, $V(\theta)$, are related by the relation

$$V(\theta) = \frac{\phi}{n} S(\theta) \cos \theta .$$

In terms of $V(\theta)$, Equations A1 to A3 can be written:

$$\Delta x = t \left[\frac{dV(\theta)}{d\theta} \cos \theta + V \sin \theta \right] \qquad (A1')$$

$$\Delta y = t \left[\sin \theta \frac{dV(\theta)}{d\theta} - V(\theta) \cos \theta \right] \qquad (A2')$$

$$Z^*(\theta) = - \left[V(\theta) + \frac{d^2V(\theta)}{d\theta^2} \right] \cdot \qquad (A3')$$

θs_1 and θs_2 are the roots of the equation $Z^*(\theta) = 0$, therefore

$$V(\theta) + \frac{d^2V(\theta)}{d\theta^2} = 0$$

with $r = 1/[V(\theta)]$ this relation becomes

$$\frac{1}{r} + \left(\frac{1}{r}\right)'' = 0 .$$

This relation means that points of geometrical inflexion are present on the curve $r(\theta)$. At these points corresponding values of θ are θs_1 and θs_2.

If ψ is the angle between the "dissolution trajectory" and the direction of ion beam we have

$$\tan \psi = \frac{\Delta x}{\Delta y} = \frac{dV(\theta)/d\theta + V(\theta) \tan \theta}{\tan \theta \, dV/d\theta - V(\theta)} \cdot \qquad (A4)$$

Let us search the values of θ for which $\tan \psi$ is extrema. We have

$$(\tan \psi)' = \frac{(\Delta x)' \Delta y - (\Delta y)' \Delta x}{(\Delta y)^2} = 0$$

with

$$(\Delta x)' = - \frac{dV(\theta)}{d\theta} \sin \theta + \frac{d^2V(\theta)}{d\theta^2} \cos \theta + \frac{dV(\theta)}{d\theta} \sin \theta + V(\theta) \cos \theta$$

$$= \cos \theta \left[V(\theta) + \frac{d^2V(\theta)}{d\theta^2} \right]$$

$$(\Delta y)' = \frac{dV(\theta)}{d\theta} \cos \theta + \frac{d^2V(\theta)}{d\theta^2} \sin \theta + V(\theta) \sin \theta - \frac{dV(\theta)}{d\theta} \cos \theta$$

$$= \sin \theta \left[V(\theta) + \frac{d^2V(\theta)}{d\theta^2} \right]$$

$(\Delta x)'$ and $(\Delta y)'$ are simultaneously equal to zero for the two values of θ : θs_1 and θs_2. Also $(\tan \psi)' = 0$ for θs_1 and θs_2. The angles ψ_1 and ψ_2 associated to θs_1 and θs_2 are the limits of the angles possible between dissolution trajectories and ion beam direction.

In Fig. 10 Δx, Δy, Z^* and $\tan \psi$ versus angle θ are drawn. It is shown that Δx, Δy and $\tan \psi$ reach extrema for the same values θs_1 and θs_2. At these points Z^* is equal to zero.

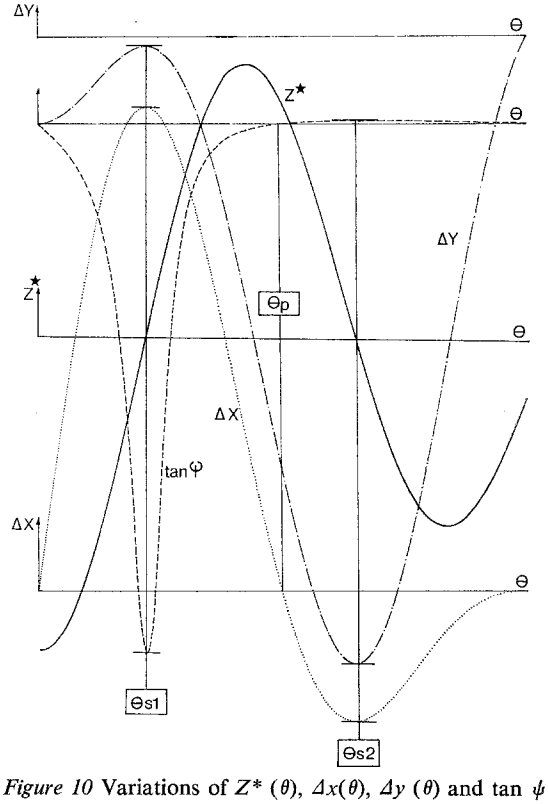

Figure 10 Variations of $Z^*(\theta)$, $\Delta x(\theta)$, $\Delta y(\theta)$ and $\tan \psi(\theta)$ versus angle of incidence θ.

References

1. A. D. G. STEWART and M. W. THOMPSON, *J. Mater. Sci.* **4** (1969) 56.
2. M. J. NOBES, J. S. COLLIGON and G. CARTER, *ibid* **4** (1969) 730.
3. G. CARTER, J. S. COLLIGON and M. J. NOBES, *ibid* **6** (1971) 115.
4. C. CATANA, J. S. COLLIGON and G. CARTER, *ibid* **7** (1972) 467.
5. G. CARTER, J. S. COLLIGON and M. J. NOBES, *ibid* **8** (1973) 473.
6. D. J. BARBER, F. C. FRANK, M. MOSS, J. W. STEEDS and I. S. T. TSONG, *ibid* **8** (1973) 1030.
7. F. C. FRANK, "Growth and Perfection of Crystals" (John Wiley, New York, 1958) p. 411.

Received 1 September and accepted 17 October 1973.